Variation of Air Circulating Velocity in Thermal Drying Oven to Reduce Energy Loss

Patsarawan Lipikanjanakul and Paisan Kittisupakorn

Abstract—**A metal can is normally used as a container in several food industries. A major problem of using the metal can as a food's container is the corrosion caused by chemical reactions between the metal can and food. Therefore, during a can making process, metal sheets are coated with food-grade lacquer and then dried in a thermal drying oven for drying evaporated solvent on the sheets surface and bonding cross linked between lacquer and the sheets. In the thermal drying oven, exhaust gas is eliminated and circulating in the oven. However, the circulating speed should be varied with respect to products' specification and production to reduce energy used resulting in cost saving of drying process. Here, a three-dimensional transient model of a thermal drying oven is generated by a computational fluid dynamics simulation program (CFD). In this work, temperature distribution velocity pattern and concentration profile studied are divided into 2 cases: a conventional one with mass flow rate 1.6667 m^3/s and the modified one with mass flow rate 1.5 m^3/s. In order to validate the model, the temperature profile from simulation of the conventional case is compared with the actual data. The result demonstrates that the model is accurate and can be applicable for studying temperature distribution, velocity pattern and concentration profile of the process. It was found that the temperature distribution at the beginning of convectional system (Case 1) more heat loss than case 2, but the average velocity of the modified system (Case 2) is lower. Moreover, the study of concentration profile shows the concentration accumulate of the modified system is slightly higher than convectional that means the process can completely dry the solvent off. Therefore, the modified system with lower circulating velocity speed can reduce heat loss of 8.84%.**

***Index Terms*— CFD simulation, temperature distribution, concentration profile, coating process**

I. Introduction

IN a metal can making process for using as a food container, it helps to keep a good quality and extend a shelf life of food products in markets. A lacquer coating is an important step for this process. Since, it helps to protect the can from the corrosion that caused by the chemical reaction between the surface and the food inside [1]. A flow chart of a metal can making process is demonstrated in Fig. 1.

Manuscript received January 10, 2015; revised February 05, 2015.:

P. Lipikanjanakul. Department of Chemical Engineering, Faculty of Engineering, Chulalongkorn University, Bangkok 10330, (e-mail: patsarawan.l@student.chula.ac.th)

P. Kittisupakorn. Department of Chemical Engineering, Faculty of Engineering, Chulalongkorn University, Bangkok 10330, (corresponding author to provide phone: 662-218-6892; fax: 662-218-6877; e-mail: paisan.k@chula.ac.th)

This process starts with a metal sheet is coated with the food-grade lacquer to protect the sheet from the corrosion and dried, it with a thermal drying oven. There are two zones appear within the oven. First is a drying zone. In this zone, the solvent in the lacquer film on the metal sheet's surface is evaporated. After the solvent is completely removed from the surface, the lacquer film is converted to a solid phase by forming the chemical bonds between the film and the surface. This latter step is called "a curing zone". After the coating section, the metal sheet is cut into a small piece by a slitting machine and constructed into a can with a designed shape, and then the metal can is tested by pressure testing or light testing method to check the can's quality before sending it to customers [2]

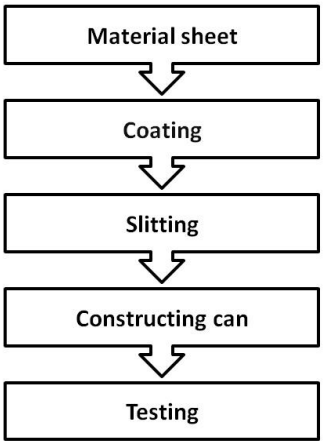

Fig. 1 Can making process

In the oven, parameters that effect to efficiency are air temperature, air velocity, time, and humidity or quantity of evaporated solvent [3]. In drying zone, temperature and time must be completely dried all solvent in the coating solution. For air velocity, this is related to diffusion and evaporated rate. Solvent medium in the lacquer, as a mention previous, is evaporated by hot air in the oven. Evaporated solvent accumulates in the oven which effect to evaporate rate. In order to reduce relative humidity of exhaust gas, the blower which is normally operated under constant rotating speed must be installed for eliminate the solvent. To reduce the operating cost, the lacquer coating step must be improved by installing an inverter to the blower in the oven for controlling an outlet air velocity in order to increase the oven efficiency.

For optimum velocity speed, an experiment installed inverter for changing a rotating speed and monitoring the temperature distribution and air pattern. This is expensive and time consuming. Therefore, computational fluid dynamics (CFD) simulation can be implemented. A model which is usually used in fluid flow is the Reynolds Averaged Navier-Stokes (RANS) that has been shown is several CFD

ISBN: 978-988-19253-2-9
ISSN: 2078-0958 (Print); ISSN: 2078-0966 (Online)

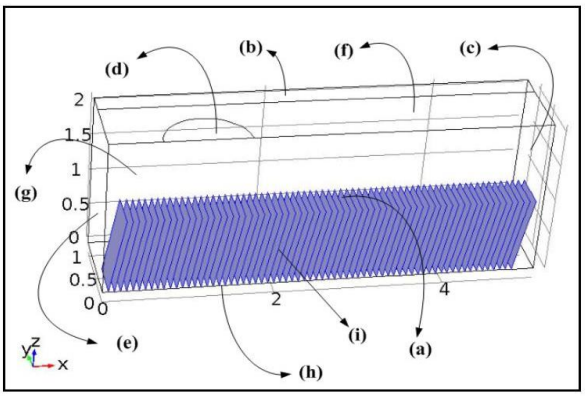

Fig. 2 Geometry of the oven

studied, for example a three-dimensional geometry simulation of a heating oven with natural air circulation [4-5], and bakery oven or bread breaking oven [6-7] etc.

This work aims to investigate the effect of the outlet air velocity on the air velocity pattern, temperature distribution in the drying zone and the concentration of evaporated solvent in the thermal drying oven by using a computational fluid dynamics simulation program (CFD) based on a three-dimensional time dependent heat transfer model with non-isothermal flow. The results from this program are validated with the real plant data to guarantee the correction of the models. In addition, this work is divided into two case studies. Case 1 is studied with the outlet air flow rate equals to 1.6667 m^3/s (Conventional system) and case 2 is studied with the outlet air flow rate equals 1.5 m^3/s (Modified system).

II. Oven Configuration

This work based on a continuous indirect-fired oven that uses in a real plant. The CFD geometry of this oven shows in Fig. 2. The oven's dimensions are 1.2975 m width, 2.095 m height and 5.1 m length. Since, the oven's dimension is symmetry then the width of this oven can be reduced by a half of its width for using in the simulation section.

In Fig. 2, surface (a) is symmetry surface for temperature and air velocity. Surface (b) is an air inlet duct with a cross sectional area 0.292 m along the length of the oven. Surface (c) shows an interface area of drying and curing zone. The semi-circle (d) is air outlet surface with 0.602 m in diameter. It is located at 1.435 m from the entrance of the oven by surface (e). The walls of the oven are shown as the surface (f), (g), and (h). Surface (i) which are located in the oven represent the metal sheets (0.01 m × 0.005 m). Each sheet is inclined at an angle 10 degree from z-axis.

TABLE II
BOUNDARY CONDITION

Boundary	Surface*	Case 1	Case 2
Initial temperature condition		303.1500	
Mass flow rate (m^3/s)		1.6667	1.5000
Normal velocity inlet (m/s)	(b)	0.1584	0.1584
Normal velocity inlet (m/s)	(c)	0.6223	0.5498
Normal velocity outlet (m/s)	(d)	4.2104	3.7893
Temperature inlet (K)	(b)	473.1500	
Temperature inlet (K)	(c)	453.1500	
Temperature inlet (K)	(e)	303.1500	
Pressure (bar)	(e)	101314.9978	
Outlet velocity	(e)		
Outflow temperature	(d)		
Symmetry heat and flow	(a)		
Interior wall	(i)		
Thin thermal resistive layer	(i)		
Convectional heat flux	(f),(g),(h)		

* Surface boundary shown in Fig. 2

III. Mathematical Model

The model of this work is based on the Reynolds Averaged Navier-Stokes equation (RANS) [8] which is divided into 3 models; velocity model, temperature model, and concentration model. All models are conservative equations in Cartesian coordinate with time dependent. The values of parameter that use in this work are summarized in Table 1.

A. Velocity model and temperature model

The velocity and temperature models in this work are non-isothermal flow models. The general form of these models including with the conservation equations of mass, momentum and energy are shown as follow;

The equation of mass conservation

$$\frac{\partial \rho}{\partial t} + \nabla(\rho u) = 0 \tag{1}$$

The equation of momentum conservation

$$\rho \frac{\partial u}{\partial t} + \rho(u \cdot \nabla)u = -\nabla p - [\nabla \cdot \tau] + F \tag{2}$$

The equation of energy conservation

TABLE I
THE TEMPERATURE DEPENDENT PHYSICAL PARAMETERS OF ETHYLENE GLYCOL BUTYL ETHER [9]

Parameter	Function	Unit	T_{max} (K)	T_{min} (K)
Density	Ideal-gas	(kg/m^3)	-	-
Heat capacity	$C_p = 118380 + 232700\left(\frac{699.9}{T \times sinh(699.9T^{-1})}\right)^2 + 172000\left(\frac{1959.9}{T \times \cos h(1959.9T^{-1})}\right)^2$	(J/kmol·K)	298.15	1500
Thermal conductivity	$k = \frac{1.87 \times 10^{-7} T^{0.9407}}{1 + 704T^{-1}}$	(kW/m·K)	444.47	1000
Viscosity	$\mu = 3.66 \times 10^{-8} T^{0.90894}$	(kg/m·s)	199.17	1000

ISBN: 978-988-19253-2-9
ISSN: 2078-0958 (Print); ISSN: 2078-0966 (Online)

$$\rho C_p \frac{\partial T}{\partial t} + \rho C_p u \cdot \nabla T = \nabla \cdot (k \nabla T) + Q + Q_{vh} + W_p \quad (3)$$

From equation (2), the viscous force (τ) can be presented by

$$\tau = -\mu\left(\nabla u + (\nabla u)^t\right) + \left(\frac{2}{3}\mu - \mu_T\right)(\nabla \cdot u)\delta \quad (4)$$

The eddy viscosity (μ_T) in (4) can be calculated by the turbulence model. The standard k-Ɛ turbulence flow model appropriates for flow in complex geometry [5-7]. This model consists of two equation are turbulence kinetic energy (k) and viscous dissipation (Ɛ). These following equations written in:

$$\frac{\partial(\rho\kappa)}{\partial t} + \rho(u \cdot \nabla)\kappa = \nabla \cdot \left[\left(\mu + \frac{\mu_T}{\sigma_k}\right)\nabla\kappa\right] + P_k - \rho\varepsilon \quad (5)$$

$$\frac{\partial(\rho\varepsilon)}{\partial t} + \rho(u \cdot \nabla)\varepsilon = \nabla \cdot \left[\left(\mu + \frac{\mu_T}{\sigma_\varepsilon}\right)\nabla k\right] + C_{\varepsilon 1}\frac{\varepsilon}{k}P_k - C_{\varepsilon 2}\rho\frac{\varepsilon^2}{k} \quad (6)$$

Where,

$$\mu_T = \rho C_\mu \frac{\kappa^2}{\varepsilon} \quad (7)$$

$$P_k = -\mu_T\left[\nabla u : \left(\nabla u + (\nabla u)^t\right) - \frac{2}{3}(\nabla \cdot u)^2\right] - \frac{2}{3}\rho k \nabla \cdot u \quad (8)$$

To consider the problem, the boundary conditions for calculating are listed in Table II and the value of adjustable constants (C_μ, σ_k, σ_ε, $C_{\varepsilon 1}$, and $C_{\varepsilon 2}$) are 0.09, 1.00, 1.30, 1.44, and 1.92, respectively [10].

In this work, either velocity model or temperature model is simulated by using COMSOL simulation multiphysics (version 4.3b). The mesh geometry was generated in free tetrahedral. The generated mesh numbers are 777270 domain elements, 57043 boundary elements, and 5713 edge elements. The simulation study has been made based on computer with windows 7 64-bit 3.0 GHz Inter core i5 CPU and 16 GB RAM.

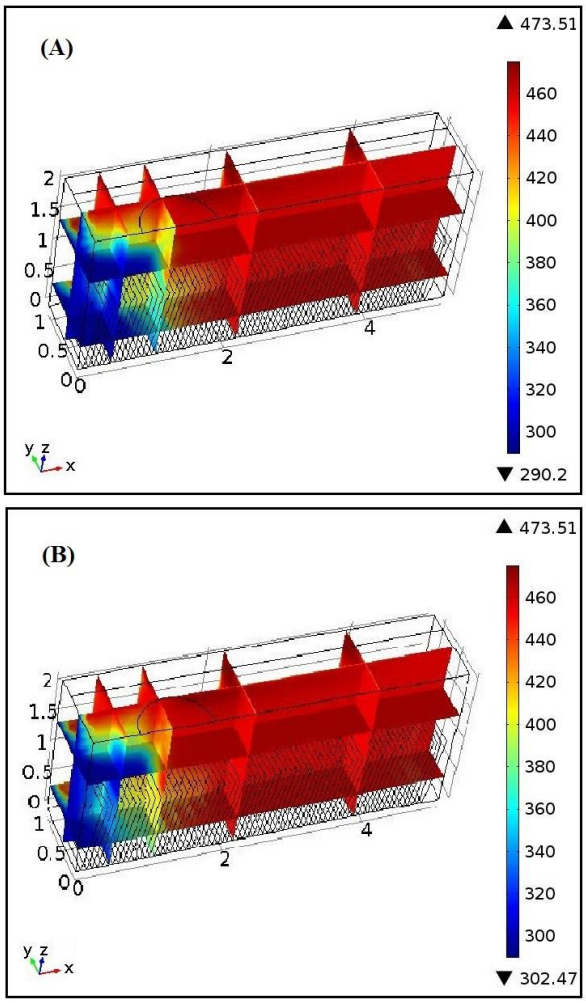

Fig. 3 Temperature distribution (A) Case 1 and (B) Case

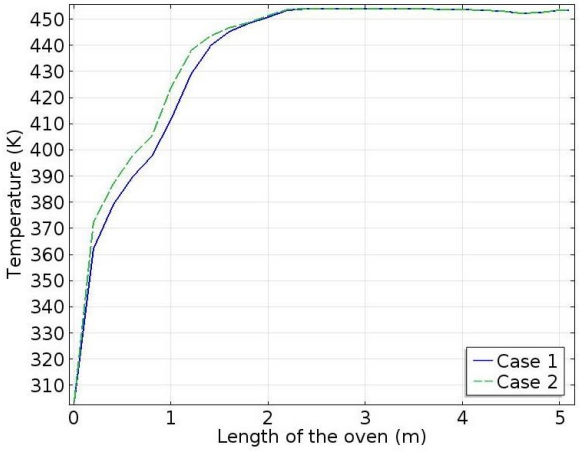

Fig. 4 Average temperature profile along the length

TABLE III
FUNCTION OF TEMPERATURE AND VELOCITY ALONG THE LENGTH

Parameter	Case	Function	R-square	Length Range Min	Length Range Max
Temperature (K)	Case 1	$-0.2925x^6 + 4.726x^5 - 29.773x^4 + 95.218x^3 - 176.63x^2 + 213.02x + 312.17$	0.9845	0.0	5.1
	Case 2	$-0.331x^6 + 5.5524x^5 - 36.649x^4 + 122.85x^3 - 230.06x^2 + 252.29x + 313.11$	0.9794	0.0	5.1
Velocity (m/s)	Case 1	$0.1469x^4 - 0.6918x^3 + 0.8461x^2 + 0.0999x + 0.3243$	0.9943	0.0	2.0
		$-0.0132x^5 + 0.1998x^4 - 1.1733x^3 + 3.3331x^2 - 4.5671x + 3.1343$	0.9719	2.0	5.1
	Case 2	$0.0863x^4 - 0.5245x^3 + 0.8415x^2 - 0.0994x + 0.3632$	0.9951	0.0	2.0
		$-0.0146x^6 + 0.2707x^5 - 2.0459x^4 + 8.0803x^3 - 17.601x^2 + 20.094x - 8.7019$	0.9924	2.0	5.1

x is length of the oven (m)

ISBN: 978-988-19253-2-9
ISSN: 2078-0958 (Print); ISSN: 2078-0966 (Online)

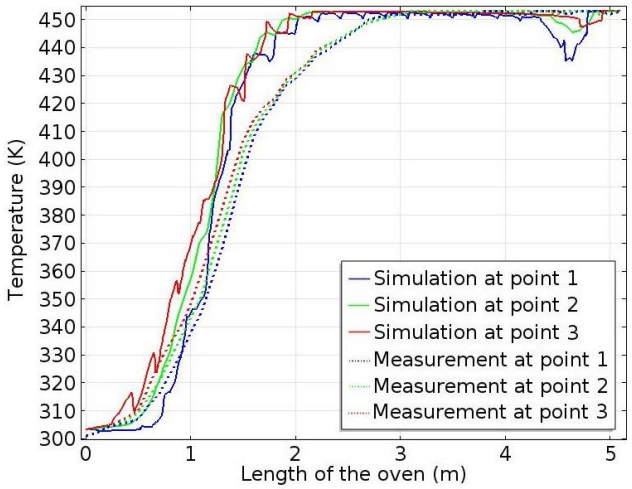

Fig. 5 Temperature comparison between simulation and measurement

The result from the temperature model is validated with the data that collected from a real plant to ensure the correction of the model. The validation points of temperature along the oven are measuring 3 points. The first point is the bottom of plate by 0.08 m × 0.08 m distance from corner. The middle of plate is a second point. For last point is on the top of the plate.

B. Concentration model

These concentration models are calculated by using MATLAB software and the value of parameters that use for calculation are obtained by the simulation results in the COMSOL software from previously section. The general form of the concentration model is shown in (9) that combine with evaporation rate [11]

$$\frac{\partial C_\alpha}{\partial t} + u \cdot \nabla C_\alpha = -(\nabla \cdot j_\alpha) + \nabla \cdot N_a \tag{9}$$

Where,

$$j_\alpha = -\alpha_{ab} \nabla C \tag{10}$$

$$\alpha_{AB} = \frac{4.14\times10^{-4} T^{1.9} \sqrt{1/MW_A + 1/MW_B}\, \mathrm{MW}_A^{-0.33}}{p} \tag{11}$$

$$N_a = k_c \Delta C \tag{12}$$

These concentration models are calculated by using MATLAB software and the value of parameters that use for calculation are obtained from the simulation results in the COMSOL software.

IV. RESULT AND DISCUSSION

A. Temperature distribution and profile

The comparison of temperature distribution in case 1 (Conventional system with the outlet air flow rate equals 1.6667 m^3/s) and case 2 (Modified system with the outlet air flow rate equals 1.5 m^3/s) at steady state is illustrated in Fig. 3. From this figure, the temperature distribution in case 1 at

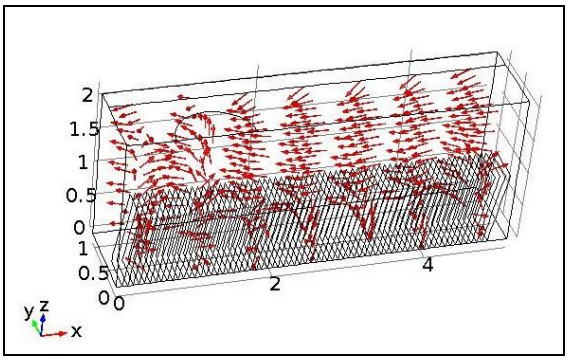

Fig. 6 Velocity pattern in the oven

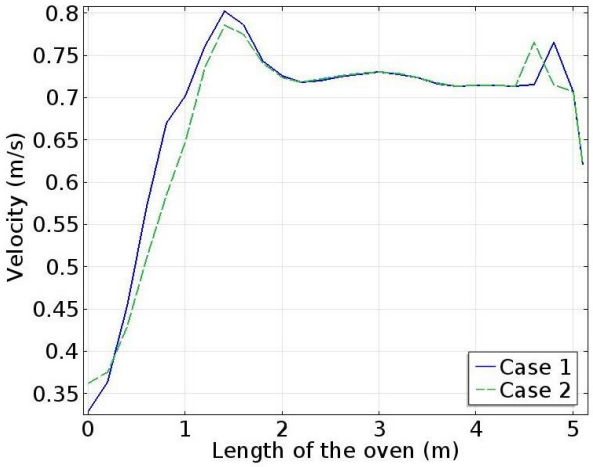

Fig. 7 Average velocity along the oven

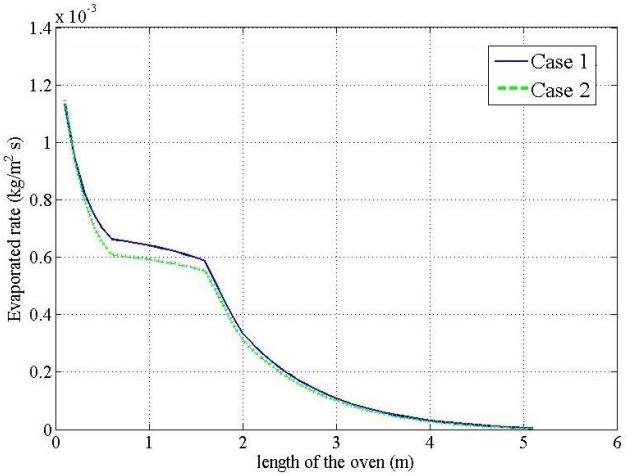

Fig. 8 Evaporated rate along the oven

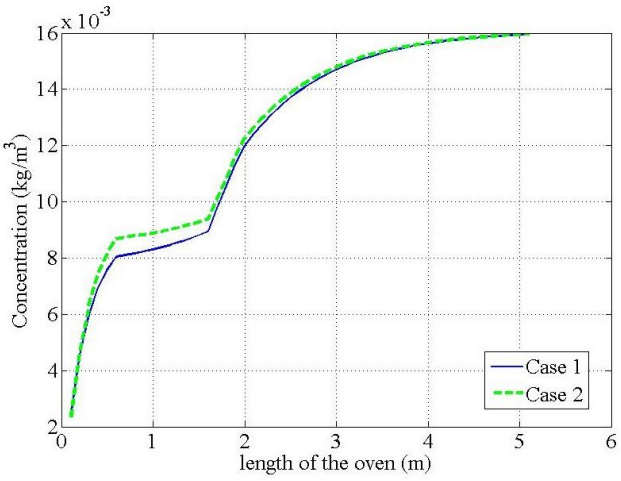

Fig. 9 Concentration along the oven

ISBN: 978-988-19253-2-9
ISSN: 2078-0958 (Print); ISSN: 2078-0966 (Online)

the entrance zone is lower than the distribution in case 2 because the average velocity in case 1 is greater than case 2, so more heat escape to surround. After that, temperature of both cases rapidly goes to control temperature at around 543 K.

For the average temperature along the oven is illustrated in Fig. 4. It can be seen that the temperature at the 0.5 m to 2 m, case 2 is higher than case 1 seeing that case 1 is more convective heat transfer to the outlet surface. Then, almost steady around 2.3 m at 453 K. At the outlet surface (b) in Fig. 2 of case 1 and case 2 are 423.1647 and 428.6035, respectively at steady state that saving heat loss around 8.84%.

Fig. 5 demonstrates that the temperature models can be used for calculation in the next section because it has a slightly different between the simulation result and the real data by less than 5%. This difference may be occurred from the error when collected the real data and simulation by assumed that sheets are not moving.

B. Velocity distribution

The velocity pattern at steady state is illustrated in Fig. 6. The both cases are insignificant difference at same model and boundary condition. Moreover profiles of average velocity along the system, both cases are similar trend as presented in Fig. 7. The maximum velocity occurs at the outlet surface of both cases. At the beginning velocity of case 1 is higher than case 2. For a peak around five meters length from the entrance, it is observed no plate around this section due to grid mesh problem that effect of the turbulence parameter, so velocity around this area is higher.

C. Concentration profile

For simulation the concentration model, the temperature and velocity functions are demonstrated in Table III by assume that the velocity and temperature is independent on time (at steady state).

The evaporation rate at steady state is illustrated in Fig. 8. The evaporation rate is mainly related to the air concentration, and then this rate is the greatest at the beginning due to less evaporated solvent in air and after that decrease until the evaporated solvent is run out. In the case 1, the evaporation rate is greater than case 2 because velocity is higher that related to convection term.

For concentration profile, evaporated rate is the main effect parameter of concentration model, then concentration is rapidly increase as shown in Fig. 9 due to result of evaporation rate. Comparison of case 1 and case 2, the trend are same but case 2 has an average concentration slightly higher than case 1 which means more accumulate solvent in the oven, but it not much effect to evaporation rate.

V. Conclusion

A three-dimensional CFD model of the transient heat transfer in a thermal drying oven is generated by using non-isothermal model. The temperature profile from simulation is compared with actual data to ensure the precision of the model and it shows that the model can be used for predicting concentration profile.

From the simulation results of temperature and velocity, the accumulated concentration in a modified system with an inverter (Case 2) is higher than that in a conventional system (Case 1) but it helps to reduce the heat loss in the drying zone by 8.84%.

Appendix

Nomenclature

C_p	specific heat capacity at constant pressure (J/(kg·K))
C_μ	turbulence model parameter
$C_{\varepsilon 1}$	turbulence model parameter
$C_{\varepsilon 2}$	turbulence model parameter
$C\alpha$	concentration of species α (kg/m^3)
F	volume force (N/m^3)
g	gravity force (m/s^2)
j_α	mass flux (kg/(m^2·s))
k	thermal conductivity (W/(m·K))
k_c	(m/s)
MW_α	molecular weight of species α (kg/mol)
Na	evaporation flux rate (kg/(m^2·s))
p	pressure (kg/(m·s^2))
P_k	Production rate of turbulence kinetic energy (J/(m^3·s))
Q	contains the heat sources (W/m^3)
Q_{vh}	viscous heating (W/m^3)
t	time (s)
T	absolute temperature (K)
u	velocity vector (m/s)
W_p	pressure work (W/m^3)
x	distance of Cartesian coordinate in x axis (m)
y	distance of Cartesian coordinate in y axis (m)
z	distance of Cartesian coordinate in z axis (m)

Greek symbols

α_{AB}	binary diffusion for system A-B (m^2/s)
ε	turbulence dissipation (J/kg)
κ	turbulence kinetic energy (J/kg)
ρ	density (kg/m3)
τ	viscous stress tensor (kg/(m·s^2))
μ	viscousity (kg/(m·s))
μ_T	eddy viscosity (kg/(m·s))
σ_k	turbulence model parameter
σ_ε	turbulence model parameter

Subscripts

x	index of Cartesian coordinate in x axis
y	index of Cartesian coordinate in y axis
z	index of Cartesian coordinate in z axis

Mathematic operations

δ	unit tensor
∇	del operator

ISBN: 978-988-19253-2-9
ISSN: 2078-0958 (Print); ISSN: 2078-0966 (Online)

ACKNOWLEDGMENT

The financial support to this work under The Institutional Research Grant (The Thailand Research Fund), IRG 5780014, and Chulalongkorn University, Contract No. RES_57_411_21_076

REFERENCES

[1] B. Othenin and Y. Pelletier, "Metallic containers for Sterilization," in *Food packaging technology, vol. 1* G. Bureau & J.-L. Multon Ed, U.S.A.: WILEY-VCH. 1996, pp. 203-219.

[2] E.P. Degarmo, J.T. Black, and R.A. Kohser, *Materials and Processes in Manufacturing*, Wiley, 2003

[3] E. Blotta, V. Balları, M. Brun, and H. Rabal, "Evaluation of speckle-interferometry descriptors to measuring drying-of-coatings," *Journal of Signal Processing*, 91, pp. 2395–2403.

[4] V.P.C. Mohan, and P. Talukdar, "Three dimensional numerical modeling of simultaneous heat and moisture transfer in a moist object subjected to convective drying," *International Journal of Heat and Mass Transfer*, *53*, pp. 4638-4650.

[5] J. Smolka, Z. Bulinski, and A.J. Nowak, "The experimental validation of a CFD model for a heating oven with natural air circulation," *Journal of Applied Thermal Engineering, 54*, pp. 387-398.

[6] M. Boulet, B. M. MarcosDostie, and C. Moresoli, "CFD modeling of heat transfer and flow field in a bakery pilot oven," *Journal of Food Engineering*, 97, pp. 393–402.

[7] M. Boulet, B. Marcos, M. Dostie, and C. Moresoli, "CFD modeling of heat transfer and flow field in a bakery pilot oven," *Journal of Food Engineering, 97*, 393–402.

[8] R.B. Bird., W.E. Stewart, and E.N. Lightfoot, *Transport phenomena*, 2nd ed., John Wiley and Sons, Inc., 2007, ch 1,3,11.

[9] C.L. Yaws, Chemical propertiea hand book. New York: MC Grew-Hill, 1999, ch 1-2, 21, 23.

[10] H.K. Versteeg, and W. Malalasekera, *An Introduction to Computational Fluid Dynamics*, 2 ed. Englant: Pearson prentice hall, 2007, ch. 3.

[11] A.A. Hummel, K.O. Braun, and M.C. Fehrenbacher, "Evaporation of a liquid in a flowing airstream," *American Industrial Hygiene Association Journal*, 57, pp 519–525, 1996.

ISBN: 978-988-19253-2-9
ISSN: 2078-0958 (Print); ISSN: 2078-0966 (Online)